Physics of Plasmas

RESEARCH ARTICLE | AUGUST 08 2023

Development of the self-modulation instability of a relativistic proton bunch in plasma

L. Verra ; S. Wyler; T. Nechaeva ; J. Pucek ; V. Bencini ; M. Bergamaschi ; L. Ranc; G. Zevi Della Porta ; E. Gschwendtner ; P. Muggli; AWAKE Collaboration; R. Agnello ; C. C. Ahdida; C. Amoedo; Y. Andrebe; O. Apsimon ; R. Apsimon ; J. M. Arnesano; P. Blanchard ; P. N. Burrows ; B. Buttenschön ; A. Caldwell ; M. Chung ; D. A. Cooke; C. Davut ; G. Demeter ; A. C. Dexter ; S. Doebert ; F. A. Elverson; J. Farmer ; A. Fasoli ; R. Fonseca ; I. Furno ; A. Gorn ; E. Granados ; M. Granetzny ; T. Graubner; O. Grulke ; E. Guran; J. Henderson ; M. Á. Kedves; S.-Y. Kim; F. Kraus ; M. Krupa ; T. Lefevre ; L. Liang; S. Liu; N. Lopes ; K. Lotov ; M. Martinez Calderon ; S. Mazzoni ; K. Moon ; P. I. Morales Guzmán ; M. Moreira ; C. Pakuza ; F. Pannell ; A. Pardons ; K. Pepitone ; E. Poimendidou; A. Pukhov ; R. L. Ramjiawan ; S. Rey; R. Rossel ; H. Saberi ; O. Schmitz ; E. Senes ; F. Silva ; L. Silva ; B. Spear ; C. Stollberg ; A. Sublet; C. Swain; A. Topaloudis ; N. Torrado ; P. Tuev ; M. Turner ; F. Velotti; V. Verzilov ; J. Vieira; M. Weidl ; C. Welsch ; M. Wendt ; M. Wing ; J. Wolfenden ; B. Woolley; G. Xia ; V. Yarygova ; M. Zepp

Phys. Plasmas 30, 083104 (2023)
https://doi.org/10.1063/5.0157391

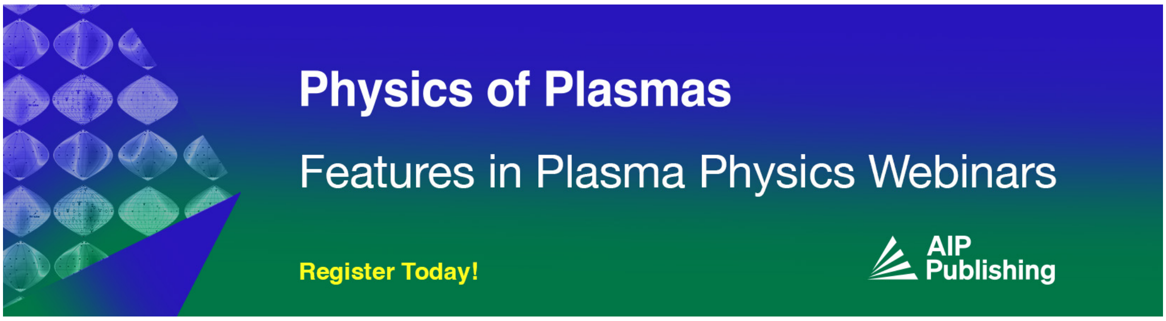

Physics of Plasmas ARTICLE pubs.aip.org/aip/pop

Development of the self-modulation instability of a relativistic proton bunch in plasma

Cite as: Phys. Plasmas **30**, 083104 (2023); doi: 10.1063/5.0157391
Submitted: 7 May 2023 · Accepted: 15 July 2023 ·
Published Online: 8 August 2023

View Online Export Citation CrossMark

L. Verra,[1,a)] S. Wyler,[2] T. Nechaeva,[3] J. Pucek,[3] V. Bencini,[1,4] M. Bergamaschi,[3] L. Ranc,[3] G. Zevi Della Porta,[1,3] E. Gschwendtner,[1] P. Muggli,[3] AWAKE Collaboration R. Agnello,[5] C. C. Ahdida,[1] C. Amoedo,[1] Y. Andrebe,[5] O. Apsimon,[6,7] R. Apsimon,[7,8] J. M. Arnesano,[1] P. Blanchard,[5] P. N. Burrows,[4] B. Buttenschön,[9] A. Caldwell,[3] M. Chung,[10] D. A. Cooke,[11] C. Davut,[6,7] G. Demeter,[12] A. C. Dexter,[7,8] S. Doebert,[1] F. A. Elverson,[1] J. Farmer,[3] A. Fasoli,[5] R. Fonseca,[13,14] I. Furno,[5] A. Gorn,[15,16] E. Granados,[1] M. Granetzny,[17] T. Graubner,[18] O. Grulke,[9,19] E. Guran,[1] J. Henderson,[7,20] M. Á. Kedves,[12] S.-Y. Kim,[1,10] F. Kraus,[18] M. Krupa,[1] T. Lefevre,[1] L. Liang,[6,7] S. Liu,[21] N. Lopes,[14] K. Lotov,[15,16] M. Martinez Calderon,[1] S. Mazzoni,[1] K. Moon,[10] P. I. Morales Guzmán,[3] M. Moreira,[14] C. Pakuza,[4] F. Pannell,[11] A. Pardons,[1] K. Pepitone,[22] E. Poimendidou,[1] A. Pukhov,[23] R. L. Ramjiawan,[1,4] S. Rey,[1] R. Rossel,[1] H. Saberi,[6,7] O. Schmitz,[17] E. Senes,[1] F. Silva,[24] L. Silva,[14] B. Spear,[4] C. Stollberg,[5] A. Sublet,[1] C. Swain,[7,25] A. Topaloudis,[1] N. Torrado,[1,14] P. Tuev,[15,16] M. Turner,[1] F. Velotti,[1] V. Verzilov,[21] J. Vieira,[14] M. Weidl,[26] C. Welsch,[7,25] M. Wendt,[1] M. Wing,[11] J. Wolfenden,[7,25] B. Woolley,[1] G. Xia,[6,7] V. Yarygova,[15,16] and M. Zepp[17]

AFFILIATIONS

[1]CERN, 1211 Geneva 23, Switzerland
[2]Ecole Polytechnique Federale de Lausanne (EPFL), Laboratory of Particle Accelerator Physics (LPAP), 1015 Lausanne, Switzerland
[3]Max Planck Institute for Physics, 80805 Munich, Germany
[4]John Adams Institute, Oxford University, Oxford OX1 3RH, United Kingdom
[5]Ecole Polytechnique Federale de Lausanne (EPFL), Swiss Plasma Center (SPC), 1015 Lausanne, Switzerland
[6]University of Manchester M13 9PL, Manchester M13 9PL, United Kingdom
[7]Cockcroft Institute, Warrington WA4 4AD, United Kingdom
[8]Lancaster University, Lancaster LA1 4YB, United Kingdom
[9]Max Planck Institute for Plasma Physics, 17491 Greifswald, Germany
[10]UNIST, Ulsan 44919, South Korea
[11]UCL, London WC1 6BT, United Kingdom
[12]Wigner Research Centre for Physics, 1121 Budapest, Hungary
[13]ISCTE – Instituto Universitéario de Lisboa, 1049-001 Lisbon, Portugal
[14]GoLP/Instituto de Plasmas e Fusão Nuclear, Instituto Superior Técnico, Universidade de Lisboa, 1049-001 Lisbon, Portugal
[15]Budker Institute of Nuclear Physics SB RAS, 630090 Novosibirsk, Russia
[16]Novosibirsk State University, 630090 Novosibirsk, Russia
[17]University of Wisconsin, Madison, Wisconsin 53706, USA
[18]Philipps-Universität Marburg, 35032 Marburg, Germany
[19]Technical University of Denmark, 2800 Kgs. Lyngby, Denmark
[20]STFC/ASTeC, Daresbury Laboratory, Warrington WA4 4AD, United Kingdom
[21]TRIUMF, Vancouver, British Columbia V6T 2A3, Canada
[22]Angstrom Laboratory, Department of Physics and Astronomy, 752 37 Uppsala, Sweden
[23]Heinrich-Heine-Universität Düsseldorf, 40225 Düsseldorf, Germany

[24]INESC-ID, Instituto Superior Técnico, Universidade de Lisboa, 1049–001 Lisbon, Portugal
[25]University of Liverpool, Liverpool L69 7ZE, United Kingdom
[26]Max Planck Institute for Plasma Physics, 80805 Garching, Germany

[a)]Author to whom correspondence should be addressed: livio.verra@cern.ch

ABSTRACT

Self-modulation is a beam–plasma instability that is useful to drive large-amplitude wakefields with bunches much longer than the plasma skin depth. We present experimental results showing that, when increasing the ratio between the initial transverse size of the bunch and the plasma skin depth, the instability occurs later along the bunch, or not at all, over a fixed plasma length because the amplitude of the initial wakefields decreases. We show cases for which self-modulation does not develop, and we introduce a simple model discussing the conditions for which it would not occur after any plasma length. Changing bunch size and plasma electron density also changes the growth rate of the instability. We discuss the impact of these results on the design of a particle accelerator based on the self-modulation instability seeded by a relativistic ionization front, such as the future upgrade of the Advanced WAKefield Experiment.

 https://doi.org/10.1063/5.0157391

I. INTRODUCTION

The self-modulation instability (SMI)[1–3] is a beam–plasma instability that can develop when a relativistic charged particle bunch, propagating in a plasma with density n_{pe}, has root mean square (rms) length σ_z much longer than the plasma skin depth c/ω_{pe}, where c is the speed of light and $\omega_{pe} = \sqrt{\frac{n_{pe}e^2}{m_e \varepsilon_0}}$ is the plasma electron angular frequency (m_e and e are the mass and charge of the electron, and ε_0 is the vacuum permittivity). When the bunch enters a preformed plasma, the features and imperfections of the initial distribution of the bunch density[4,5] drive initial wakefields[6] that act on the bunch itself. The transverse component of these wakefields generates a periodic focusing and defocusing force, modulating the radius of the bunch. Since the longitudinal relative motion of highly relativistic particles due to the action of the longitudinal component of the wakefields is negligible, the modulation of the radius results in a longitudinal modulation of the bunch density.

The instability grows exponentially from the initial modulation, and microbunches form on the axis when the effect of the focusing force becomes significant when compared to the natural divergence of the bunch. According to the linear theory,[1,7,8] the amplitude of the transverse wakefields $W_\perp$ grows along the plasma (z) and along the bunch (t), starting from the initial amplitude $W_{\perp 0}(t)$, as $W_\perp(z,t) = W_{\perp 0}(t)\exp(\Gamma(z,t)z)$, where Γ is the growth rate of the instability. As the instability grows along the bunch, the full modulation into microbunches first occurs late along the Gaussian bunch and progressively reaches its front during propagation in plasma. Thus, the effect of Γ is smaller at the front than at the back[1,7,8] ($\Gamma \propto t^{1/3}$).

Once the bunch is fully modulated into a train of microbunches (i.e., SMI reaches saturation), it resonantly drives wakefields that can be used for high-gradient particle acceleration.[9] The development of SMI may be ensured and made reproducible by seeding[4,10,11] or may be suppressed by decreasing the amplitude of the initial wakefields.

In the context of the Advanced WAKefield Experiment (AWAKE) at CERN,[12] we previously demonstrated that a long, Gaussian, relativistic proton (p^+) bunch undergoes the self-modulation process in plasma[2,3] and that externally injected electrons can be accelerated to GeV-energies.[9] We also showed that self-modulation can be seeded by a relativistic ionization front (RIF) copropagating within the p^+ bunch[4] or by wakefields driven by a preceding, short electron bunch.[10] In the case of RIF seeding, seed wakefields are provided by the fast onset of the beam–plasma interaction at the location of the RIF.

The possibility of varying the initial parameters of the bunch and plasma allows for further studies on the development of SMI. In previous experiments, we showed that the growth rate of the instability increases when increasing n_{pe}[3] or when increasing the peak bunch charge density n_{b0}.[10] It is also interesting to measure the dependence of the amplitude of the initial transverse wakefields and of the development of the instability on initial parameters. When $W_{\perp 0}$ is decreased, it takes a longer propagation distance in plasma for the initial modulation to form and, therefore, for SMI to grow. Thus, the earliest time along the bunch where SMI is observed is a probe for $W_{\perp 0}$, which causes the initial modulation.

We perform experiments in which the bunch density is much lower than the plasma density ($n_{b0}/n_{pe} < 0.08$ in all cases), and therefore initial wakefields are in the linear regime. The amplitude of the initial transverse wakefields is proportional to n_{b0} and inversely proportional to the ratio between the initial rms transverse size of the bunch[13] σ_{r0} and c/ω_{pe} ($W_{\perp 0} \propto n_{b0}(c/\omega_{pe})^2 \propto (c/\omega_{pe})^2/\sigma_{r0}^2$), as the wakefields are defined by the amount of bunch charge contained within c/ω_{pe}. Hence, when increasing σ_{r0} (keeping constant the charge and the other parameters of the bunch), both $W_{\perp 0}$ and Γ decrease[1,7,8] ($\Gamma \propto \omega_{pe}(tn_{b0}/n_{pe})^{(1/3)}$), resulting in a smaller amplitude of the wakefields during the growth of SMI, and eventually, in the suppression of the development of the instability. When increasing n_{pe}, $W_{\perp 0}$ decreases, whereas Γ increases.[1,3,7,8]

In this paper, we present experimental results showing that, when increasing σ_{r0} or n_{pe}, the modulation becomes observable only later along the bunch, due to a lower $W_{\perp 0}$, because the amplitude of the wakefields necessary to make protons converge on the axis is reached later. We also discuss cases for which this condition may not be reached before the density peak of the bunch, and therefore, SMI may not take place.

We perform the experiments by measuring the charge density distribution of the bunch on time-resolved images obtained after propagation in plasma. The occurrence of SMI may be directly visible from time-resolved images and, with higher sensitivity, from the power spectrum of the discrete Fourier transform of their on-axis profile. In particular, we show that the development of SMI can be controlled, delayed, and even suppressed by varying these initial parameters.

We also discuss the implications for the design of a plasma wakefield accelerator based on the self-modulation of the drive bunch.

In a potential upgrade of AWAKE,[14,15] SMI will be made reproducible by seeding it in a first plasma with a RIF. In this case, the part of the bunch ahead of the RIF will keep propagating in vapor, diverging as in a vacuum. Then, the bunch will enter preformed plasma (the accelerator) after a gap region where the on-axis injection of the witness electron bunch will take place.[16] Therefore, for high-quality acceleration, it will be necessary that the front of the bunch does not undergo SMI in the second plasma and does not interfere with the wakefields driven by the (seeded) self-modulated part of the bunch.

II. EXPERIMENTAL SETUP

In AWAKE (Fig. 1), the plasma is generated by ionizing rubidium vapor contained in a 10-m-long source with an $\sim$120 fs, $\sim$100 mJ laser pulse focused to a radius of $\sim$1 mm.[17] The vapor density n_{vap} is controlled by varying the temperature of the reservoirs containing the rubidium and of the vapor source.[18] Previous experimental results showed that the laser pulse singly ionizes all the rubidium atoms on its path,[2] thus, $n_{pe} = n_{vap}$. In the experiments presented here, we use $n_{pe} = 0.97 \times 10^{14}$ cm^{-3} and $n_{pe} = 7.3 \times 10^{14}$ cm^{-3}, which we refer to as low and high plasma electron densities in the following. The CERN Super-Proton Synchrotron (SPS) delivers the 44.9 nC, $\sigma_z = 6.3$ cm bunch of 400 GeV/c protons.[19] The final focusing system of the transport line provides flexibility for placing the waist of the beam at different locations z^* with respect to the plasma entrance ($z = 0$) and for varying the transverse size σ_{r0} of the bunch entering the plasma. By changing n_{pe} and σ_{r0}, we, therefore, vary the ratio $\sigma_{r0}/(c/\omega_{pe}) \propto \sigma_{r0}\sqrt{n_{pe}}$, and thus, the amplitude of the initial wakefields as well as the growth rate of the self-modulation process.

The transverse size of the beam at different locations along the beamline is measured on screens (yellow trapezoids in Fig. 1) emitting optical transition radiation (OTR) when the bunch traverses them. The OTR is transported and imaged onto the chip of CMOS cameras, producing time-integrated images of the p^+ bunch transverse distribution. The light produced by one of these screens, positioned 3.5 m downstream of the plasma exit ($z = 13.5$ m), is also sent to a streak camera, producing a time-resolved image of the p^+ bunch charge density distribution in a 180-μm-wide slice (the spatial resolution of the optical system[20]) near the propagation axis of the bunch.

Figures 2(a) and 2(b) show the time-integrated, transverse distribution of the bunch at the screen closest to the plasma entrance [$z = -1.5$ m, second measurement location in Fig. 2(c)] for two sets of beam transport optics configurations, which we hereafter refer to as narrow and wide-bunch optics, respectively. Fitting the transverse projections (black lines) with a Gaussian distribution, we calculate the transverse size of the beam in the two planes (x, y) as the rms $\sigma_{x,y}$. The transverse size is also confirmed to be constant along the bunch using time-resolved images.[10] By fitting $\sigma_{x,y}$ measured without plasma at the various screens along the propagation axis z [Fig. 2(c)] with the solution of the beam envelope equation in vacuum $\sigma_{x,y}(z) = \sigma^*_{x,y}\sqrt{1 + (z - z^*_{x,y})^2\left(\frac{\varepsilon_{x,y}/(\beta\gamma)}{\sigma^*_{x,y}{}^2}\right)^2}$, we obtain the transverse size at the waist $\sigma^*_{x,y}$, the waist position $z^*_{x,y}$, and the normalized transverse emittance $\varepsilon_{x,y}$ (β is the ratio between bunch longitudinal velocity and c, and γ is the Lorentz factor). We then calculate the size of the beam at the plasma entrance $\sigma_{x,y}(z = 0)$. For the narrow-bunch optics [circles in Fig. 2(c); blue: x-plane, red: y-plane; dashed lines: envelope equation fits], $\sigma^*_{x,y} = (0.19, 0.18)$ mm, $\varepsilon_{x,y} = (2.9, 2.7)$ mm-mrad, and the waist position is close to the plasma entrance: $z^*_{x,y} = (-2.6, -2.9)$ m (smaller than the Twiss parameter $\beta^*_{x,y} = \sigma^{*2}_{x,y}\beta\gamma/\varepsilon_{x,y} = (5.3, 4.6)$ m), and $\sigma_{x,y}(z = 0) = (0.21, 0.21)$ mm. For the wide-bunch optics [crosses and dotted lines in Fig. 2(c)], $z^*_{x,y} = (-9.4, -10.8)$ m,

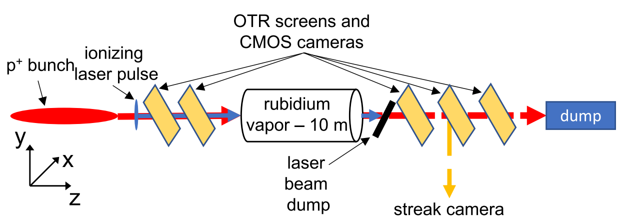

FIG. 1. Schematic of the AWAKE experimental setup: the ionizing laser pulse (blue) enters the 10-m-long vapor source (white cylinder) ahead of the p^+ bunch (red) and singly ionizes the rubidium atoms, creating the plasma. The optical transition radiation produced by aluminum-coated screens (yellow trapezoids) when the bunch enters them is imaged onto the chip of CMOS cameras, producing time-integrated images [e.g., Figs. 2(a) and 2(b)] or on the entrance slit of a streak camera, producing time-resolved images (e.g., Fig. 3). The two screens upstream of the vapor source are extracted from the beamline during experiments with plasma.

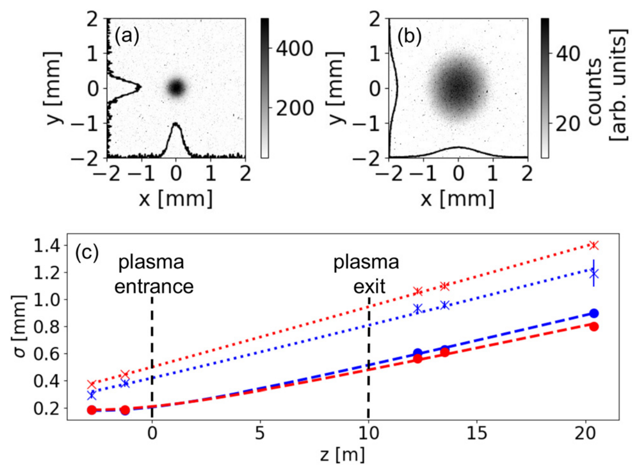

FIG. 2. Transverse, time-integrated images (x, y) of (a) the narrow and (b) wide bunch, at $z = -1.5$ m. Black lines show the projections of the transverse planes. (c) The transverse size of the bunch along the beamline $\sigma_{x,y}$, obtained from Gaussian, fits to the transverse projections of images at the various screens with no plasma. Circles: narrow-bunch optics, crosses: wide-bunch optics, blue symbols: x-plane, red symbols: y-plane. Dashed and dotted lines: the result of the fits with the envelope equation. Plasma entrance at $z = 0$, exit at $z = 10$ m.

with same emittance, and size at the waist as with the narrow bunch. This means that the waist is located about $2\beta^*_{x,y}$ upstream of the plasma entrance. Thus, in this case, the bunch enters the plasma diverging and with transverse size $\sigma_{x,y} = (0.42, 0.50)$ mm. The uncertainties on the parameters of the fits are given in Ref. 21. As the difference in size between the two planes is smaller than the difference between the two optical settings, and it does not influence the results presented here, in the following, we quote the average of the values in the two planes as σ_{r0}.

III. EXPERIMENTAL RESULTS

Figure 3(a) shows a single-event, time-resolved ns timescale image of the narrow p^+ bunch after propagation in vapor (no laser pulse, thus no plasma: bunch propagates as in vacuum), representing the incoming bunch as observed at the screen positioned 3.5 m downstream of the vapor source exit. The temporal [blue line in Fig. 3(c)] and spatial [black line in Fig. 3(a)] projections show that the bunch has a 2D-Gaussian charge density profile. After propagation in plasma with $n_{pe} = 0.97 \times 10^{14}$ cm^{-3} ($\sigma_{r0}/(c/\omega_{pe}) = 0.39$ at the plasma entrance [see Fig. 3(b)], the spatial projection (black line) is no longer Gaussian because of the occurrence of SMI: the microbunch train generates the bright core[2] and the defocused protons generate the surrounding halo.[3]

In this experiment, the laser pulse propagates $\sim$1 ns ahead of the p^+ bunch center ($\sim$4.7 σ_z/c), hence self-modulation occurs as an instability (i.e., no timing nor amplitude reproducibility of the wakefields) because the bunch density at the location of the ionization front is too low to seed.[4] The time resolution of ns timescale images ($\sim$5 ps[20]) is not sufficient to resolve the microbunch structure at this plasma electron density (plasma electron period $T_{pe} = 2\pi/\omega_{pe} = 11.3$ ps). Hence,

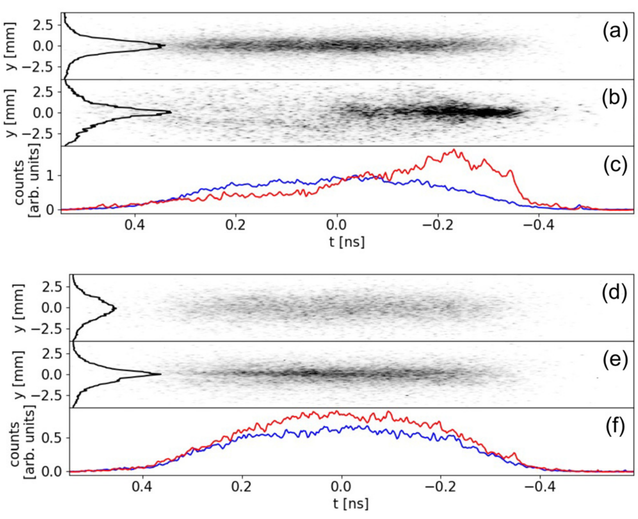

FIG. 3. Single-event, time-resolved images of the p^+ bunch at the screen at $z = 13.5$ m. (a) and (b): narrow bunch; (d) and (e): wide bunch. (a) and (d): after propagation without plasma; (b) and (e): after propagation with plasma. (c) and (f): time projections of the narrow and wide bunch, respectively, obtained by summing the counts along the y-spatial direction. Black lines along the vertical axes: spatial projections. Blue lines: without plasma, red lines: with plasma. The duration of the streak camera window is 1.1 ns. The bunch propagates from left to right; bunch center at $t = 0$. Same color scale for all images. $n_{pe} = 0.97 \times 10^{14}$ cm^{-3}.

the charge distribution appears continuous. The transverse extent of the distribution along the bunch depends on the transverse momentum acquired by the defocused protons during the growth of the instability.[10,22] It is, therefore, a probe for the amplitude of the wakefields at the early stage of SMI. The effect of the entrance slit of the streak camera is to decrease the intensity of the time-resolved images where the transverse extent of the distribution increases (the amount of charge per time slice remains constant).[23] The time projection of the image with plasma [Fig. 3(c), red line] shows this effect by the higher count values at the front of the bunch ($-0.4 \lesssim t \lesssim -0.1$ ns) than the projection of the image without plasma (blue line), because the bunch is focused by the adiabatic response of the plasma[10] and because of the formation of the microbunch train. Conversely, the rapid decrease later along the bunch observed at the screen ($t > -0.2$ ns) is due to defocusing from the occurrence of SMI, causing the transverse extent of the bunch to increase.[10] The decrease in the signal on the axis, later along the bunch, is also due to dephasing between the microbunch train and the wakefields[7,8,24] and the divergence of protons between the plasma exit and the screen.

In the case of the wide bunch (the charge and the other parameters of the bunch are kept constant), the image without plasma [Fig. 3(d)] is less bright than for the narrow bunch [Fig. 3(a), the streak camera settings are the same for all images]. The spatial projection in the case with plasma [Fig. 3(e), black line; $\sigma_{r0}/(c/\omega_{pe}) = 0.85$] is peaked and no longer Gaussian. We attribute the peaked transverse distribution of Fig. 3(e) to SMI, as confirmed later with ps timescale images (Fig. 6). A quantitative comparison of the two distributions is not performed because the total number of counts of the images changes due to the effect of the slit. The time projection of the case with plasma [Fig. 3(f), red line] does not show a rapid decrease in counts along the bunch as in (c), indicating a weaker effect of SMI on the bunch and thus that the average amplitude of the transverse wakefields is much smaller than in the case of the narrow bunch. In fact, in Fig. 3(e), there is no clear evidence of the surrounding halo distribution visible in Fig. 3(b). This is expected because the smaller n_{b0} and larger $\sigma_{r0}/(c/\omega_{pe})$ lead to smaller amplitude of the initial wakefields $W_{\perp 0}$ and smaller growth rate Γ.[3,10]

In secs. III A–III D, we use a shorter streak camera time window (210 ps), providing a better time resolution ($\sim$2 ps) to evidence the microbunch train itself (if any) with a narrow and wide bunch in low and high plasma electron densities.

A. Narrow bunch, low plasma electron density

We observe the charge density distribution at the front of the bunch to investigate the position along the bunch where the modulation becomes detectable. Figure 4(a) shows six consecutive, single-event, time-resolved images of the narrow p^+ bunch: one after propagation without plasma (#1) and five after propagation with plasma (#2 − 6), between 180 and 360 ps ahead of the bunch center. The images are aligned in time with sub-ps precision using an optical timing fiducial.[25] The on-axis profile of the event without plasma (blue line) shows the increase in the intensity along the Gaussian distribution of the bunch and no periodic oscillation. On the contrary, the microbunch structure is clearly visible on all events with plasma, and the corresponding on-axis profiles [e.g., red line, the profile of event #6 on Fig. 4(a)] show a periodic modulation. Images show that the timing

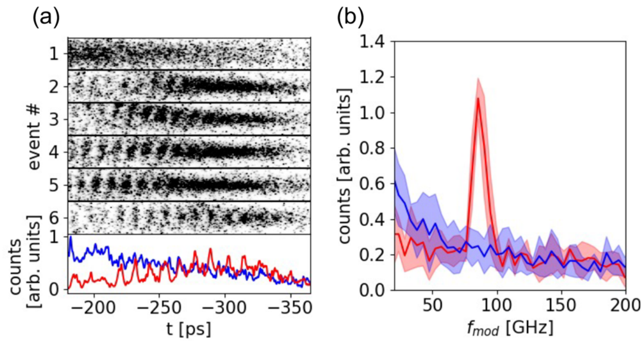

FIG. 4. (a) Six time-resolved, consecutive, single-event images of the narrow p^+ bunch. Event #1: without plasma; events #2 – 6: with plasma. Blue line: on-axis profile of event #1; red line: on-axis profile of event #6. The counts are normalized with respect to the maximum projection of the image without plasma. The duration of the streak camera window is 210 ps. The width of each image is $\Delta y = \pm 1.25$ mm centered on the beam propagation axis. (b) Average power spectra obtained from the DFT of the on-axis profiles of single-event images. Red line: average of the power spectra of five consecutive events with plasma [events #2 – 6 from (a)]; blue line: average of the power spectra of five consecutive events without plasma (including event #1). The shaded areas show the extent of the rms variations. Same color scale for all images. $n_{pe} = 0.97 \times 10^{14}$ cm^{-3}, $f_{pe} = 88.3$ GHz.

of the modulation is not reproducible from event to event because the instability is not seeded.[4]

To measure the frequency of the modulation f_{mod}, we perform a discrete Fourier transform (DFT) of the on-axis profiles of the single-event images, such as those of Fig. 4(a). Figure 4(b) shows the average power spectra for five events with plasma (red line) and five events without plasma (blue line), together with their rms variation as the corresponding shaded areas. The spectrum of the events with plasma is clearly peaked at $f_{mod} = 85 \pm 5$ GHz (the uncertainty is estimated as the width of a frequency bin), which is consistent with the expected plasma electron frequency $f_{pe} = \omega_{pe}/2\pi = 88.3$ GHz. The signal-to-noise ratio, defined as the ratio between the peak value at f_{mod} and the corresponding value for the spectrum without plasma, plus its rms, is close to three. This indicates that the modulation depth of the profiles due to SMI is much larger than that due to the random variation in the distribution of the signal without plasma, as visible from the time-resolved images and profiles. Hence, after 10 m of propagation in plasma at this location along the bunch, the microbunches are clearly visible, indicating that the instability has taken place.

B. Wide bunch, low plasma electron density

In the case of the wide bunch [Fig. 5(a)] and over the same time range as for the narrow bunch [Fig. 4(a)], the microbunches are not distinguishable on time-resolved images. The absence of the occurrence of SMI is also confirmed by the DFT analysis, which shows very similar power spectra with and without plasma [see Fig. 5(b)], i.e., without a detectable peak at the expected $f_{mod} \sim f_{pe}$. This indicates that, if present, the periodic modulation due to SMI is not deeper than the variation due to noise in the distribution of the images obtained without plasma.

We estimate the modulation depth of the bunch density necessary to create a peak in the power spectrum above the noise level: we determine the amplitude of a sinusoidal modulation on a smooth,

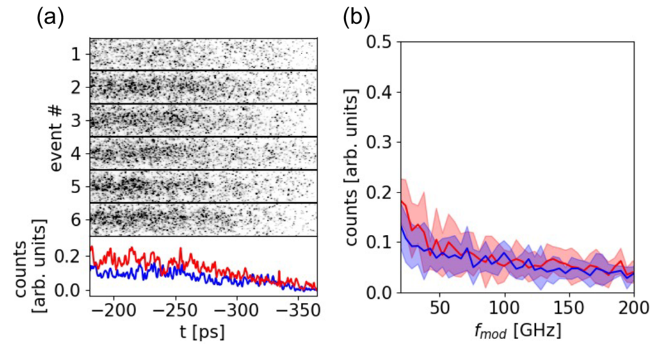

FIG. 5. Same as Fig. 4, for the wide p^+ bunch.

ideal Gaussian distribution whose power spectrum near f_{pe} has an amplitude equal to twice the rms variation of the spectrum of the events without plasma. In the case of Fig. 5(b), the limit for detection of the modulation depth due to SMI is $\sim$20 %. For comparison, according to the same simple model, the peak of the power spectrum of the narrow bunch [Fig. 4(b)] corresponds to an amplitude of the sinusoidal component >40 %, with a detection threshold of $\sim$15 %.

Figure 6(a) shows that, with the same wide bunch, microbunches do become visible later along the bunch [$-240 \le t \le -60$ ps, rather than $-360 \le t \le -180$ ps, as in Fig. 4(a)]. The average power spectrum [red line, Fig. 6(b)] shows a clear peak above the noise level at $f_{mod} \sim f_{pe}$, indicating a modulation depth around four times larger than the minimum detectable value ($\sim$15 %, estimated as for Fig. 5).

This confirms that SMI also takes place with the wide bunch [as already suggested by the spatial projection of Fig. 3(e)], but it is observed only later along the bunch than with the narrow bunch. This is because the amplitude of the initial wakefields $W_{\perp 0}$ is smaller, with the smaller n_{b0} and larger $\sigma_{r0}/(c/\omega_{pe})$. This also indicates a longer saturation length of the instability as well as a lower amplitude of the wakefields driven by the bunch at any given location along the plasma and bunch.

C. High plasma electron density

The plasma skin depth shortens when increasing n_{pe}. Thus, for a fixed transverse size of the drive bunch, the ratio $\sigma_{r0}/(c/\omega_{pe})$ increases, less bunch charge is contained within c/ω_{pe}, and the

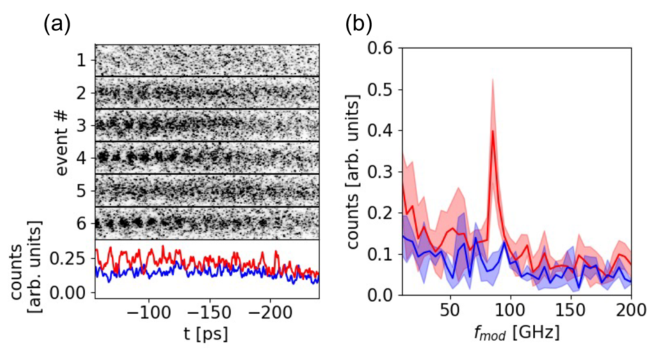

FIG. 6. Same as Fig. 5, for a later time range along the wide p^+ bunch.

amplitude of the initial wakefields $W_{\perp 0}$ decreases. We acquire time-resolved images of the bunch with $n_{pe} = 7.3 \times 10^{14}$ cm^{-3} in a 73 ps time window, with sufficient time resolution ($\sim$1 ps) to detect modulation at the expected $f_{pe} = 242.3$ GHz ($T_{pe} = 4.13$ ps) at the expense of a lower signal-to-noise ratio because of lower counts per pixel. Single images do not show evidence of SMI due to the limited time resolution. We therefore only use the more sensitive DFT method to assess the occurrence of SMI.[26] Figure 7(a) shows that the average power spectrum obtained from time-resolved images of the narrow bunch in plasma ($\sigma_{r0}/(c/\omega_{pe}) = 1.1$, red line) at $-370 \leq t \leq -300$ ps (i.e., shorter than but within the same time range as Fig. 4) does not have a peak with amplitude significantly larger than the level of the average spectrum of the events without plasma (blue). This indicates a possible modulation depth no larger than the initial rms variation of the bunch density distribution ($\sim$20 %).

At $-220 \leq t \leq -150$ ps [i.e., later along the bunch, Fig. 7(b)], the average power spectrum of the images with plasma is clearly peaked at $f_{mod} = 246 \pm 14$ GHz $\sim f_{pe}$. The uncertainty is larger than in the previous cases because the observation window is shorter. Observing a peak in the power spectrum confirms that the lower $W_{\perp 0}$ causes a later development of SMI along the bunch.

With the wide bunch [Fig. 7(c)], there is no visible peak at f_{pe} with amplitude higher than the threshold ($\sim$20 %) in the same late time window as for (b), indicating again that lower n_{b0} and larger $\sigma_{r0}/(c/\omega_{pe})$ delay the development of the microbunch train along the bunch. To further investigate whether the wide bunch undergoes SMI

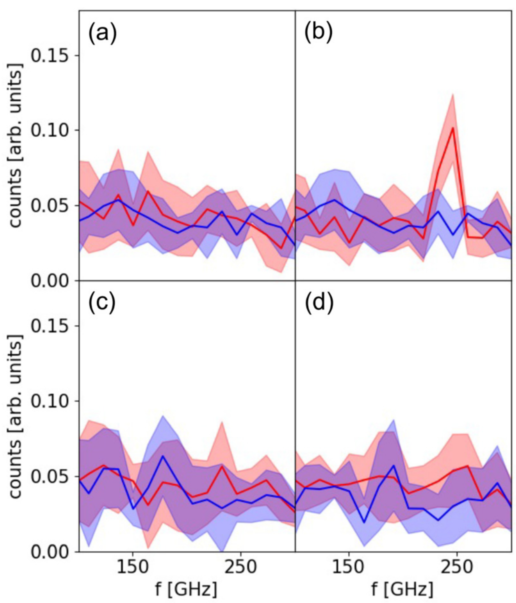

FIG. 7. Average power spectra from the DFT analysis on the on-axis profiles of single-events images. Red lines: average of five consecutive events with plasma; blue lines: average of five consecutive events without plasma. The shaded areas show the extent of the corresponding rms variations. The duration of the streak camera window is 73 ps for all cases. (a) Narrow bunch, measuring between $t = -300$ and -370 ps (early). (b) Narrow bunch, measuring between $t = -150$ and -220 ps (late). (c) Wide bunch, measuring between $t = -150$ and -220 ps. (d) Wide bunch, RIF at the bunch center, measuring between $t = +170$ and $+240$ ps (i.e., after the center of the bunch). $n_{pe} = 7.3 \times 10^{14}$ cm^{-3}, $f_{pe} = 242.3$ GHz.

at all in high-density plasma, we also measure the charge density distribution when the ionization front propagates at the center of the bunch, i.e., we impose the maximum possible amplitude of the initial wakefields (RIF seeding). Figure 7(d) shows that no peak at f_{pe} in the average power spectrum of the events with plasma is distinguishable from the power spectrum of the events without plasma ($+170 \leq t \leq +240$ ps). Therefore, we conclude that at this high density, the wide bunch does not self-modulate at all over 10 m, even when SMI is strongly seeded. In this case, $\sigma_{r0}/(c/\omega_{pe}) = 2.4 > 1$, which means that the plasma return current can flow through the bunch, and current filamentation instability[27,28] could develop. Further experiments to study this phenomenon and its effects are under way.[29]

D. Summary of the experimental results

Previous measurements[4] indicate that SMI "starts" at a location along a Gaussian bunch where a perturbation of, or imperfection in the bunch density (on a spatial scale $\ll c/\omega_{pe}$), limited by the local bunch density, is sufficient to initiate the process. This occurs where the amplitude of the wakefields that the perturbation drives are sufficient for the resulting transverse force to overcome the effect of the divergence of the slice with finite emittance. While each slice of the bunch, with the same radius and emittance, diverges at the same rate at the entrance of the plasma, the amplitude of wakefields that can be driven increases from the front of the bunch till its peak. One can estimate a first position along the bunch where SMI may occur by using the amplitude of wakefields driven if there were a sharp step in the bunch density at the location of the slice. In this case, the amplitude $W_{\perp 0}$ can be calculated as was done in Ref. 4 using the linear wakefield theory, since $n_{b0} \ll n_{pe}$. This is equivalent to using an envelope equation for each slice at the entrance of the plasma,

$$\sigma_r'' = \left(\frac{\varepsilon_g^2}{\sigma_{r0}^3} - \frac{eW_{\perp 0}}{\gamma m_e c^2} \right), \qquad (1)$$

where $W_{\perp 0}(t) = 2 \frac{e n_{b0}}{\varepsilon_0 k_{pe}^2} \exp(-t/2\sigma_z^2) dR/dr|_{r=\sigma_{r0}}$. The $R(r)$ coefficient is a function of the transverse bunch profile and describes the radial dependence of the wakefields.[13] The position along the bunch where SMI can first develop from can be calculated by setting the RHS of Eq. (1) to zero to find the equivalent of a matching condition. For each slice ahead of it, the effect of divergence dominates (i.e., RHS > 0), and SMI cannot develop. For each slice behind it, RHS <0 and SMI can develop. In particular, in the case of a bunch for which the "matched" condition cannot be met before the peak of the bunch, SMI can never develop. This is because the focusing force generated by diverging slices decreases with propagation distance ($W_{\perp}(z) \propto n_{b0}(z) \propto 1/\sigma_r^2(z)$), ensuring that past the plasma entrance, SMI never develops ahead of the "matched" slice, unlike in the classical case of focusing in a pure ion column where the force remains constant upon propagation.[30,31] Thus, diverging slices keep diverging with distance. This is confirmed by the cases of Fig. 7(c), for which SMI does not develop, and Fig. 7(d), for which it does not even with the strongest possible $W_{\perp 0}$ (note that in this case, the bunch is not at a waist at the plasma entrance).

We summarize the results in Fig. 8 by schematically displaying what was observed in each time window (blue circles: SMI, continuous

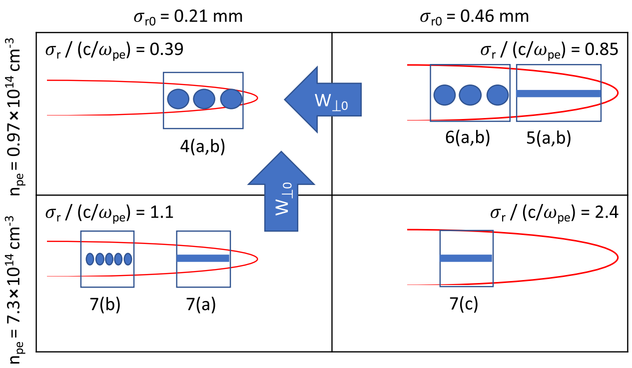

FIG. 8. Schematic summary of the experimental results. The red half ellipses represent the p^+ bunch traveling from left to right, and the blue rectangles represent the streak camera windows where measurements were performed. Blue circles: SMI observed in the window; blue lines: SMI not observed. The blue arrows indicate how $W_{\perp 0}$ varies with σ_{r0} (horizontal direction) and with n_{pe} (vertical direction).

line: no SMI) from time-resolved images and from their DFT power spectrum (i.e., detecting or not a peak corresponding to the modulation). The results indicate that the earliest time along the bunch where SMI is observed depends on the amplitude of the initial wakefields $W_{\perp 0}$, in agreement with what is suggested by the simple model we presented. When increasing the transverse size of the bunch (horizontal direction in the schematic) or when increasing the plasma electron density (vertical direction), the amplitude of the initial wakefields decreases. Regardless of the growth rate, SMI can only occur where and when the initial wakefields overcome the divergence of the bunch. However, as noted, noise in the time-resolved images imposes a detection limitation. Thus, even though SMI is not detected, it may be present at a level lower than the detection threshold.

IV. IMPACT ON THE ACCELERATOR DESIGN

To effectively employ the p^+-driven scheme for accelerator applications, the timing and amplitude of the wakefields must be reproducible from event to event because the witness bunch must be deterministically injected in the accelerating and focusing phase of the wakefields with sub-ps accuracy for every event. Reproducibility is obtained by seeding the instability,[4,10,11] i.e., driving initial wakefields with sufficient amplitude for SMI to grow from. In the case of RIF seeding, a transition from the instability to the seeded regime was observed when the local bunch density at the RIF location overcomes a threshold value.[4] For the narrow bunch, we measured the transition to occur between 400 and 300 ps ahead of the bunch center (not shown here).

With the experiments presented in this paper, we replicate with the wide bunch and a single plasma the conditions of the bunch front entering the second plasma, with a large initial transverse size and similar divergence. The results show that the radial and longitudinal intensity modulation ahead of the transition point for RIF seeding[4] does not reach a depth distinguishable from that of the incoming bunch distribution [see Figs. 5 and 7(c)] after propagation in the 10-m-long plasma that corresponds to the second plasma of the accelerator setup. This suggests that acceleration driven only by the self-modulated back part of the bunch can proceed without interference caused by the SMI of the front of the bunch in the second plasma.[32] This is a necessary condition for producing a high-quality accelerated bunch with this scheme. The acceleration experiments with the two plasma sections are anyway needed to prove that neither SMI nor CFI occurs in the second plasma.

V. CONCLUSIONS

We showed with experimental results that the condition for SMI to develop along a long p^+ bunch depends on the amplitude of the initial wakefields that the bunch can drive. This amplitude decreases when increasing the ratio $\sigma_{r0}/(c/\omega_{pe}) \propto \sigma_{r0}\sqrt{n_{pe}}$. We observed that SMI appears later along the bunch when increasing the initial transverse size of the bunch or the plasma electron density and does not occur (within the detection threshold) when increasing both. Measurements also confirmed that when increasing the initial transverse size σ_{r0} (thus, decreasing n_{b0}) while keeping the other parameters constant, the growth rate Γ of the self-modulation instability (when this occurs) decreases.

We discussed the impact of these results on the design of a p^+-driven plasma wakefield accelerator based on the self-modulation instability seeded by a copropagating relativistic ionization front. We showed that, for a diverging bunch with a large transverse size (comparable to that of the bunch front left unmodulated from a first plasma where seeding occurs), the modulation at the bunch front does not reach a detectable depth ahead of the transition point for RIF seeding.

ACKNOWLEDGMENTS

This work was supported in parts by STFC (AWAKE-UK, Cockcroft Institute core, John Adams Institute core, and UCL consolidated grants), United Kingdom and the National Research Foundation of Korea (Nos. NRF-2016R1A5A1013277 and NRF-2020R1A2C1010835). M. Wing acknowledges the support of DESY, Hamburg. The support of the National Office for Research, Development and Innovation (NKFIH) under contract numbers 2019-2.1.6-NEMZ_KI-2019-00004, and the support of the Wigner Datacenter Cloud facility through the Awakelaser project is acknowledged. TRIUMF contribution is supported by NSERC of Canada. The AWAKE collaboration acknowledges the SPS team for their excellent proton delivery.

AUTHOR DECLARATIONS

Conflict of Interest

The authors have no conflicts to disclose.

Author Contributions

Livio Verra: Conceptualization (lead); Formal analysis (lead); Investigation (lead); Resources (equal); Visualization (lead); Writing – original draft (lead). **Samuel Wyler:** Investigation (equal); Resources (equal). **Tatiana Nechaeva:** Investigation (equal); Resources (equal). **Jan Pucek:** Investigation (equal); Resources (equal). **Vittorio Bencini:** Investigation (equal); Resources (equal). **Michele Bergamaschi:** Investigation (equal); Resources (equal). **Lucas Ranc:** Investigation (equal); Resources (equal). **Giovanni Zevi Della Porta:** Investigation (equal); Project administration (equal); Resources (equal). **Edda Gschwendtner:** Funding acquisition (equal); Project administration (equal); Resources (equal); Supervision (equal). **Patric Muggli:** Conceptualization (lead); Formal analysis (equal); Investigation (lead); Resources (equal); Supervision (equal); Writing – original draft (lead). **Riccardo Agnello:** Resources (equal). **Claudia Christina Ahdida:** Resources (equal). **Carolina Amoedo:** Resources (equal). **Yanis Andrebe:** Resources (equal). **Oznur Mete Apsimon:** Resources (equal). **Rob Apsimon:** Resources (equal). **Jordan Arnesano:** Resources (equal). **Patrick Blanchard:** Resources (equal). **Philip Burrows:** Resources (equal). **Birger Buttenschön:** Resources (equal). **Allen Caldwell:** Resources (equal). **Moses Chung:** Resources (equal). **David Cooke:** Resources (equal). **Can Davut:** Resources (equal). **Gabor Demeter:** Resources (equal). **Amos Christopher Dexter:** Resources (equal). **Steffen Doebert:** Resources (equal). **Francesca Elverson:** Resources (equal). **John Patrick Farmer:** Resources (equal). **Ambrogio F. Fasoli:** Resources (equal). **Ricardo Fonseca:** Resources (equal). **Ivo Furno:** Resources (equal). **Alexander Andreevich Gorn:** Resources (equal). **Eduardo Granados:** Resources (equal). **Marcel Granetzny:** Resources (equal). **Tim Graubner:** Resources (equal). **Olaf Grulke:** Resources (equal). **Eloise Daria Guran:** Resources (equal). **James Henderson:** Resources (equal). **Miklos Kedves:** Resources (equal). **Seong-Yeol Kim:** Resources (equal). **Florian Kraus:** Resources (equal). **Michal Krupa:** Resources (equal). **Thibaut Lefevre:** Resources (equal). **Linbo Liang:** Resources (equal). **Shengli Liu:** Resources (equal). **Nelson Lopes:** Resources (equal). **Konstantin V. Lotov:** Resources (equal). **Miguel Martinez Calderon:** Resources (equal). **Stefano Mazzoni:** Resources (equal). **Kook-Jin Moon:** Resources (equal). **Pablo Morales Guzman:** Resources (equal). **Mariana Moreira:** Resources (equal). **Collette Pakuza:** Resources (equal). **Fern Pannell:** Resources (equal). **Ans Pardons:** Resources (equal). **Kevin Pepitone:** Resources (equal). **Eirini Poimendidou:** Resources (equal). **Alexander Pukhov:** Resources (equal). **Rebecca Ramjiawan:** Resources (equal). **Stephane Rey:** Resources (equal). **Ralf E Rossel:** Resources (equal). **Hossein Saberi:** Resources (equal). **Oliver Schmitz:** Resources (equal). **Eugenio Senes:** Resources (equal). **Fernando Silva:** Resources (equal). **Luis Silva:** Resources (equal). **Bethany Jane Spear:** Resources (equal). **Christine Stollberg:** Resources (equal). **Alban Sublet:** Resources (equal). **Catherine Swain:** Resources (equal). **Athanasios Topaloudis:** Resources (equal). **Nuno Torrado:** Resources (equal). **Petr V. Tuev:** Resources (equal). **Marlene Turner:** Resources (equal). **Francesco Velotti:** Resources (equal). **Victor Verzilov:** Resources (equal). **Jorge Vieira:** Resources (equal). **Martin S. Weidl:** Resources (equal). **Carsten Peter Welsch:** Resources (equal). **Manfred Wendt:** Resources (equal). **Matthew Wing:** Resources (equal). **Joseph Wolfenden:** Resources (equal). **Benjamin Woolley:** Resources (equal). **Guoxing Xia:** Resources (equal). **Vlada Yarygova:** Resources (equal). **Michael Zepp:** Resources (equal).

DATA AVAILABILITY

The data that support the findings of this study are available from the corresponding author upon reasonable request.

REFERENCES

[1] N. Kumar, A. Pukhov, and K. Lotov, "Self-modulation instability of a long proton bunch in plasmas," Phys. Rev. Lett. **104**, 255003 (2010).

[2] AWAKE Collaboration, "Experimental observation of proton bunch modulation in a plasma at varying plasma densities," Phys. Rev. Lett. **122**, 054802 (2019).

[3] M. Turner, E. Adli, A. Ahuja, O. Apsimon, R. Apsimon, A.-M. Bachmann, M. Barros Marin, D. Barrientos, F. Batsch, J. Batkiewicz, J. Bauche, V. K. Berglyd Olsen, M. Bernardini, B. Biskup, A. Boccardi, T. Bogey, T. Bohl, C. Bracco, F. Braunmüller, S. Burger, G. Burt, S. Bustamante, B. Buttenschön, A. Caldwell, M. Cascella, J. Chappell, E. Chevallay, M. Chung, D. Cooke, H. Damerau, L. Deacon, L. H. Deubner, A. Dexter, S. Doebert, J. Farmer, V. N. Fedosseev, G. Fior, R. Fiorito, R. A. Fonseca, F. Friebel, L. Garolfi, S. Gessner, I. Gorgisyan, A. A. Gorn, E. Granados, O. Grulke, E. Gschwendtner, A. Guerrero, J. Hansen, A. Helm, J. R. Henderson, C. Hessler, W. Hofle, M. Hüther, M. Ibison, L. Jensen, S. Jolly, F. Keeble, S.-Y. Kim, F. Kraus, T. Lefevre, G. LeGodec, Y. Li, S. Liu, N. Lopes, K. V. Lotov, L. Maricalva Brun, M. Martyanov, S. Mazzoni, D. Medina Godoy, V. A. Minakov, J. Mitchell, J. C. Molendijk, R. Mompo, J. T. Moody, M. Moreira, P. Muggli, E. Öz, E. Ozturk, C. Mutin, C. Pasquino, A. Pardons, F. Peña Asmus, K. Pepitone, A. Perera, A. Petrenko, S. Pitman, G. Plyushchev, A. Pukhov, S. Rey, K. Rieger, H. Ruhl, J. S. Schmidt, I. A. Shalimova, E. Shaposhnikova, P. Sherwood, L. O. Silva, L. Soby, A. P. Sosedkin, R. Speroni, R. I. Spitsyn, P. V. Tuev, F. Velotti, L. Verra, V. A. Verzilov, J. Vieira, H. Vincke, C. P. Welsch, B. Williamson, M. Wing, B. Woolley, and G. Xia (AWAKE Collaboration), "Experimental observation of plasma wakefield growth driven by the seeded self-modulation of a proton bunch," Phys. Rev. Lett. **122**, 054801 (2019).

[4] F. Batsch, P. Muggli, R. Agnello, C. C. Ahdida, M. C. Amoedo Goncalves, Y. Andrebe, O. Apsimon, R. Apsimon, A.-M. Bachmann, M. A. Baistrukov, P. Blanchard, F. Braunmüller, P. N. Burrows, B. Buttenschön, A. Caldwell, J. Chappell, E. Chevallay, M. Chung, D. A. Cooke, H. Damerau, C. Davut, G. Demeter, H. L. Deubner, S. Doebert, J. Farmer, A. Fasoli, V. N. Fedosseev, R. Fiorito, R. A. Fonseca, F. Friebel, I. Furno, L. Garolfi, S. Gessner, I. Gorgisyan, A. A. Gorn, E. Granados, M. Granetzny, T. Graubner, O. Grulke, E. Gschwendtner, V. Hafych, A. Helm, J. R. Henderson, M. Hüther, I. Y. Kargapolov, S.-Y. Kim, F. Kraus, M. Krupa, T. Lefevre, L. Liang, S. Liu, N. Lopes, K. V. Lotov, M. Martyanov, S. Mazzoni, D. Medina Godoy, V. A. Minakov, J. T. Moody, K. Moon, P. I. Morales Guzmán, M. Moreira, T. Nechaeva, E. Nowak, C. Pakuza, H. Panuganti, A. Pardons, A. Perera, J. Pucek, A. Pukhov, R. L. Ramjiawan, S. Rey, K. Rieger, O. Schmitz, E. Senes, L. O. Silva, R. Speroni, R. I. Spitsyn, C. Stollberg, A. Sublet, A. Topaloudis, N. Torrado, P. V. Tuev, M. Turner, F. Velotti, L. Verra, V. A. Verzilov, J. Vieira, H. Vincke, C. P. Welsch, M. Wendt, M. Wing, P. Wiwattananon, J. Wolfenden, B. Woolley, G. Xia, M. Zepp, and G. Z. D. Porta (AWAKE Collaboration), "Transition between instability and seeded self-modulation of a relativistic particle bunch in plasma," Phys. Rev. Lett. **126**, 164802 (2021).

[5] K. V. Lotov, G. Z. Lotova, V. I. Lotov, A. Upadhyay, T. Tückmantel, A. Pukhov, and A. Caldwell, "Natural noise and external wakefield seeding in a proton-driven plasma accelerator," Phys. Rev. Spec. Top. Accel. Beams **16**, 041301 (2013).

[6] P. Chen, J. M. Dawson, R. W. Huff, and T. Katsouleas, "Acceleration of electrons by the interaction of a bunched electron beam with a plasma," Phys. Rev. Lett. **54**, 693–696 (1985).

[7] A. Pukhov, N. Kumar, T. Tückmantel, A. Upadhyay, K. Lotov, P. Muggli, V. Khudik, C. Siemon, and G. Shvets, "Phase velocity and particle injection in a self-modulated proton-driven plasma wakefield accelerator," Phys. Rev. Lett. **107**, 145003 (2011).

[8] C. B. Schroeder, C. Benedetti, E. Esarey, F. J. Grüner, and W. P. Leemans, "Growth and phase velocity of self-modulated beam-driven plasma waves," Phys. Rev. Lett. **107**, 145002 (2011).

[9] AWAKE Collaboration, "Acceleration of electrons in the plasma wakefield of a proton bunch," Nature **561**, 363–367 (2018).

[10] L. Verra, G. Z. D. Porta, J. Pucek, T. Nechaeva, S. Wyler, M. Bergamaschi, E. Senes, E. Guran, J. T. Moody, M. A. Kedves, E. Gschwendtner, P. Muggli, R. Agnello, C. C. Ahdida, M. C. A. Goncalves, Y. Andrebe, O. Apsimon, R. Apsimon, J. M. Arnesano, A.-M. Bachmann, D. Barrientos, F. Batsch, V. Bencini, P. Blanchard, P. N. Burrows, B. Buttenschön, A. Caldwell, J. Chappell, E. Chevallay, M. Chung, D. A. Cooke, C. Davut, G. Demeter, A. C. Dexter, S. Doebert, F. A. Elverson, J. Farmer, A. Fasoli, V. Fedosseev, R. Fonseca, I. Furno, A. Gorn, E. Granados, M. Granetzny, T. Graubner, O. Grulke, V. Hafych, J. Henderson, M. Hüther, V. Khudiakov, S.-Y. Kim, F. Kraus, M. Krupa, T. Lefevre, L. Liang, S. Liu, N. Lopes, K. Lotov, M. Martinez Calderon, S. Mazzoni, D. Medina Godoy, K. Moon, P. I. Morales Guzmán, M. Moreira, E.

Nowak, C. Pakuza, H. Panuganti, A. Pardons, K. Pepitone, A. Perera, A. Pukhov, R. L. Ramjiawan, S. Rey, O. Schmitz, F. Silva, L. Silva, C. Stollberg, A. Sublet, C. Swain, A. Topaloudis, N. Torrado, P. Tuev, F. Velotti, V. Verzilov, J. Vieira, M. Weidl, C. Welsch, M. Wendt, M. Wing, J. Wolfenden, B. Woolley, G. Xia, V. Yarygova, and M. Zepp (AWAKE Collaboration), "Controlled growth of the self-modulation of a relativistic proton bunch in plasma," Phys. Rev. Lett. **129**, 024802 (2022).

[11]Y. Fang, V. E. Yakimenko, M. Babzien, M. Fedurin, K. P. Kusche, R. Malone, J. Vieira, W. B. Mori, and P. Muggli, "Seeding of self-modulation instability of a long electron bunch in a plasma," Phys. Rev. Lett. **112**, 045001 (2014).

[12]P. Muggli, E. Adli, R. Apsimon, F. Asmus, R. Baartman, A.-M. Bachmann, M. B. Marin, F. Batsch, J. Bauche, V. K. B. Olsen, M. Bernardini, B. Biskup, E. B. Vinuela, A. Boccardi, T. Bogey, T. Bohl, C. Bracco, F. Braunmuller, S. Burger, G. Burt, S. Bustamante, B. Buttenschön, A. Butterworth, A. Caldwell, M. Cascella, E. Chevallay, M. Chung, H. Damerau, L. Deacon, A. Dexter, P. Dirksen, S. Doebert, J. Farmer, V. Fedosseev, T. Feniet, G. Fior, R. Fiorito, R. Fonseca, F. Friebel, P. Gander, S. Gessner, I. Gorgisyan, A. A. Gorn, O. Grulke, E. Gschwendtner, A. Guerrero, J. Hansen, C. Hessler, W. Hofle, J. Holloway, M. Hüther, M. Ibison, M. R. Islam, L. Jensen, S. Jolly, M. Kasim, F. Keeble, S.-Y. Kim, F. Kraus, A. Lasheen, T. Lefevre, G. LeGodec, Y. Li, S. Liu, N. Lopes, K. V. Lotov, M. Martyanov, S. Mazzoni, D. M. Godoy, O. Mete, V. A. Minakov, R. Mompo, J. Moody, M. T. Moreira, J. Mitchell, C. Mutin, P. Norreys, E. Öz, E. Ozturk, W. Pauw, A. Pardons, C. Pasquino, K. Pepitone, A. Petrenko, S. Pitmann, G. Plyushchev, A. Pukhov, K. Rieger, H. Ruhl, J. Schmidt, I. A. Shalimova, E. Shaposhnikova, P. Sherwood, L. Silva, A. P. Sosedkin, R. Speroni, R. I. Spitsyn, K. Szczurek, J. Thomas, P. V. Tuev, M. Turner, V. Verzilov, J. Vieira, H. Vincke, C. P. Welsch, B. Williamson, M. Wing, G. Xia, and H. Zhang (AWAKE Collaboration), "AWAKE readiness for the study of the seeded self-modulation of a 400 GeV proton bunch," Plasma Phys. Controlled Fusion **60**, 014046 (2017).

[13]R. Keinigs and M. E. Jones, "Two-dimensional dynamics of the plasma wake-field accelerator," Phys. Fluids **30**, 252–263 (1987).

[14]E. Gschwendtner, "Awake Run 2 at CERN," in International Particle Accelerator Conference, IPAC'21, Paper No. TUPAB159 (2021).

[15]P. Muggli, "Physics to plan AWAKE Run 2," J. Phys. **1596**, 012008 (2020).

[16]L. Verra, E. Gschwendtner, and P. Muggli, "Study of external electron beam injection into proton driven plasma wakefields for AWAKE Run 2," J. Phys. **1596**, 012007 (2020).

[17]G. Demeter, J. T. Moody, M. A. Kedves, B. Ráczkevi, M. Aladi, A.-M. Bachmann, F. Batsch, F. Braunmüller, G. P. Djotyan, V. Fedosseev, F. Friebel, S. Gessner, E. Granados, E. Guran, M. Hüther, V. Lee, M. Martyanov, P. Muggli, E. Öz, H. Panuganti, L. Verra, and G. Z. Della Porta, "Long-range propagation of ultrafast ionizing laser pulses in a resonant nonlinear medium," Phys. Rev. A **104**, 033506 (2021).

[18]G. Plyushchev, R. Kersevan, A. Petrenko, and P. Muggli, "A rubidium vapor source for a plasma source for awake," J. Phys. D **51**, 025203 (2017).

[19]J. S. Schmidt, D. Barrientos, M. Barros Marin, B. Biskup, A. Boccardi, T. B. Bogey, T. Bohl, C. Bracco, S. Cettour Cave, H. Damerau *et al.*, "AWAKE Proton Beam Commissioning," in International Particle Accelerator Conference, IPAC'17, Paper No. TUPIK032 (2017).

[20]T. Nechaeva, L. Verra, G. Z. D. Porta, and P. Muggli, "A method for obtaining 3D charge density distribution of a self-modulated proton bunch," J. Phys. **2420**, 012063 (2023).

[21]The uncertainty on each parameter of the fits is obtained from the covariance matrix. For all cases shown in Fig. 2(c), the uncertainty on $\sigma^*_{x,y}$ is $<12\,\mu$m, on $\varepsilon_{x,y}$ is <0.2 mm-mrad, on $z^*_{x,y}$ is <0.8 m.

[22]M. Turner, P. Muggli, E. Adli, R. Agnello, M. Aladi, Y. Andrebe, O. Apsimon, R. Apsimon, A.-M. Bachmann, M. A. Baistrukov, F. Batsch, M. Bergamaschi, P. Blanchard, P. N. Burrows, B. Buttenschön, A. Caldwell, J. Chappell, E. Chevallay, M. Chung, D. A. Cooke, H. Damerau, C. Davut, G. Demeter, L. H. Deubner, A. Dexter, G. P. Djotyan, S. Doebert, J. Farmer, A. Fasoli, V. N. Fedosseev, R. Fiorito, R. A. Fonseca, F. Friebel, I. Furno, L. Garolfi, S. Gessner, B. Goddard, I. Gorgisyan, A. A. Gorn, E. Granados, M. Granetzny, O. Grulke, E. Gschwendtner, V. Hafych, A. Hartin, A. Helm, J. R. Henderson, A. Howling, M. Hüther, R. Jacquier, S. Jolly, I. Y. Kargapolov, M. A. Kedves, F. Keeble, M. D. Kelisani, S.-Y. Kim, F. Kraus, M. Krupa, T. Lefevre, Y. Li, L. Liang, S. Liu, N. Lopes, K. V. Lotov, M. Martyanov, S. Mazzoni, D. Medina Godoy, V. A. Minakov, J. T. Moody, P. I. Morales Guzmán, M. Moreira, H. Panuganti, A. Pardons, F. Peña Asmus, A. Perera, A. Petrenko, J. Pucek, A. Pukhov, B. Ráczkevi, R. L. Ramjiawan, S. Rey, H. Ruhl, H. Saberi, O. Schmitz, E. Senes, P. Sherwood, L. O. Silva, P. V. Tuev, F. Velotti, L. Verra, V. A. Verzilov, J. Vieira, C. P. Welsch, B. Williamson, M. Wing, J. Wolfenden, B. Woolley, G. Xia, M. Zepp, and G. Z. D. Porta (AWAKE Collaboration), "Experimental study of wakefields driven by a self-modulating proton bunch in plasma," Phys. Rev. Accel. Beams **23**, 081302 (2020).

[23]A.-M. Bachmann and P. Muggli, "Determination of the charge per micro-bunch of a self-modulated proton bunch using a streak camera," J. Phys. **1596**, 012005 (2020).

[24]F. Braunmüller, T. Nechaeva, E. Adli, R. Agnello, M. Aladi, Y. Andrebe, O. Apsimon, R. Apsimon, A.-M. Bachmann, M. A. Baistrukov, F. Batsch, M. Bergamaschi, P. Blanchard, P. N. Burrows, B. Buttenschön, A. Caldwell, J. Chappell, E. Chevallay, M. Chung, D. A. Cooke, H. Damerau, C. Davut, G. Demeter, L. H. Deubner, A. Dexter, G. P. Djotyan, S. Doebert, J. Farmer, A. Fasoli, V. N. Fedosseev, R. Fiorito, R. A. Fonseca, F. Friebel, I. Furno, L. Garolfi, S. Gessner, B. Goddard, I. Gorgisyan, A. A. Gorn, E. Granados, M. Granetzny, O. Grulke, E. Gschwendtner, V. Hafych, A. Hartin, A. Helm, J. R. Henderson, A. Howling, M. Hüther, R. Jacquier, S. Jolly, I. Y. Kargapolov, M. A. Kedves, F. Keeble, M. D. Kelisani, S.-Y. Kim, F. Kraus, M. Krupa, T. Lefevre, Y. Li, L. Liang, S. Liu, N. Lopes, K. V. Lotov, M. Martyanov, S. Mazzoni, D. Medina Godoy, V. A. Minakov, J. T. Moody, P. I. Morales Guzmán, M. Moreira, P. Muggli, H. Panuganti, A. Pardons, F. Peña Asmus, A. Perera, A. Petrenko, J. Pucek, A. Pukhov, B. Ráczkevi, R. L. Ramjiawan, S. Rey, H. Ruhl, H. Saberi, O. Schmitz, E. Senes, P. Sherwood, L. O. Silva, R. I. Spitsyn, P. V. Tuev, M. Turner, F. Velotti, L. Verra, V. A. Verzilov, J. Vieira, C. P. Welsch, B. Williamson, M. Wing, J. Wolfenden, B. Woolley, G. Xia, M. Zepp, and G. Z. D. Porta (AWAKE Collaboration), "Proton bunch self-modulation in plasma with density gradient," Phys. Rev. Lett. **125**, 264801 (2020).

[25]F. Batsch, "Setup and characteristics of a timing reference signal with sub-ps accuracy for AWAKE," J. Phys. **1596**, 012006 (2020).

[26]K. Rieger, A. Caldwell, O. Reimann, R. Tarkeshian, and P. Muggli, "GHz modulation detection using a streak camera: Suitability of streak cameras in the AWAKE experiment," Rev. Sci. Instrum. **88**, 025110 (2017).

[27]R. Lee and M. Lampe, "Electromagnetic instabilities, filamentation, and focusing of relativistic electron beams," Phys. Rev. Lett. **31**, 1390–1393 (1973).

[28]B. Allen, V. Yakimenko, M. Babzien, M. Fedurin, K. Kusche, and P. Muggli, "Experimental study of current filamentation instability," Phys. Rev. Lett. **109**, 185007 (2012).

[29]P. Muggli, L. Verra, N. Lopes, and A. Sublet, "Self-modulation and current filamentation instabilities of long and wide proton bunches in plasma," in 14th International Particle Accelerator Conference, IPAC '23 (2023).

[30]J. B. Rosenzweig, "Nonlinear plasma dynamics in the plasma wake-field accelerator," Phys. Rev. Lett. **58**, 555–558 (1987).

[31]P. Muggli, B. E. Blue, C. E. Clayton, S. Deng, F.-J. Decker, M. J. Hogan, C. Huang, R. Iverson, C. Joshi, T. C. Katsouleas, S. Lee, W. Lu, K. A. Marsh, W. B. Mori, C. L. O'Connell, P. Raimondi, R. Siemann, and D. Walz, "Meter-scale plasma-wakefield accelerator driven by a matched electron beam," Phys. Rev. Lett. **93**, 014802 (2004).

[32]M. A. Baistrukov and K. V. Lotov, "Evolution of equilibrium particle beams in plasma under external wakefields," Plasma Phys. Controlled Fusion **64**, 075003 (2022).